Performance of Femtocell Access Point Deployments in User Hot-Spot Scenarios

Martin Taranetz, Markus Rupp

Vienna University of Technology, Institute of Telecommunications
Gusshausstrasse 25/389, A-1040 Vienna, Austria
Email: {mtaranet, mrupp}@nt.tuwien.ac.at

***Abstract*—In this work, we investigate the impact of user clustering on the performance of femtocell-enhanced macrocellular networks. Various *degrees of clustering* are evaluated: A low degree corresponds to almost uniform user distributions, whereas a high degree relates to densly populated user hot-spots. Clustered user-scenarios are generated by applying a Poisson cluster process. We start out with a plain macrocellular network and cover an increasing amount of these clusters by femtocells. Expressions for the achieved Signal-to-Interference Ratio (SIR) of macrocell- and femtocell users are formulated and evaluated numerically. The efficiency of the femtocell enhancement is quantified by means of sum spectral efficiency and fairness.**

***Index Terms*—Femtocells, Femtocell Deployment, Femtocell Density, User Hot-spot, Spectral Efficiency, Sum Spectral Efficiency, Fairness, Fairness Index**

I. Introduction and Contributions

Spatial frequency reuse is one of the key methods to sustain the ever increasing demand for capacity in today's mobile cellular networks. However, high spatial reuse and thus, small cell sizes can hardly be realized in current macrocellular deployments. This led to the emergence of heterogeneous networks, which contain various types of access nodes and pose new challenges for the design of appropriate system models. The authors of [1–4] propose to apply stochastic geometry for modeling the spatial distribution of base stations and users.

A. Motivation

- While the main focus of current research lies on the positioning of the transmitters, users are commonly considered uniformly distributed [1, 3–5]. However, Femtocell Access Points (FAPs), which is a recent development of short-range low-cost low-power base stations, are most effectively deployed at user hot-spots [6, 7]. Therefore, appropriate models for the user distribution are essential to investigate the performance limits of a heterogeneous network.
- Extensive system level simulations with femtocell-enhanced macrocellular networks have been carried out. However, the employed system models are often too elaborated to precisely trace back the origin of particular effects.

B. Contributions

- We set up a system model based on stochastic geometry, which allows us to explicitely analyze the impact of various *degrees of user clustering*.
- User clusters are distributed uniformly over the area. We start out with a plain macrocellular network and investigate the effects of covering an increasing amount of randomly chosen clusters by FAPs.
- We stress the importance of a fairness metric, which is often disregarded in literature. Sum spectral efficiency provides only limited view on the user performance, since it conceals the distribution of the users' individual spectral efficiency values. Severe imbalances can particularly appear in heterogeneous cellular networks, like the one investigated in this paper.

C. Outline

The paper is organized as follows: Section II introduces the system model and presents the generation of user hot-spot scenarios. Analytic expressions for the occurring Signal-to-Interference Ratios (SIRs) are provided in Section III. Then, Section IV sets up a simulation environment and discusses the obtained results for SIR distribution, spectral efficiency and fairness. Section V concludes the work.

II. System Setup

We refer to the system model of [7] and extend it to the sectorized case. The values assigned to the different parameters for simulation are described in Section IV.

A. Cell Geometry (see Figure 1)

- The macrocellular network is composed of a central site and one tier of neighbors. Each site employs three BSs with directional antennas. The main radiation directions are spaced out 120°.
- FAPs are equipped with omni-directional antennas.
- Each FAP is assumed to be surrounded by an indoor area of radius R_I. The separation between indoor areas and outdoor environment is modeled by a wall penetration loss L.

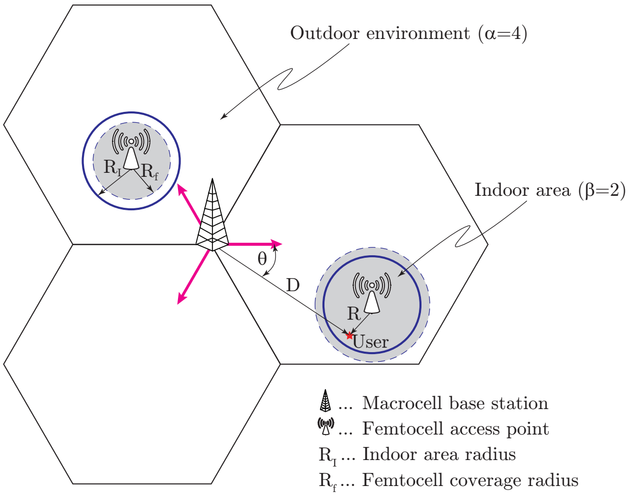

Fig. 1: System model geometry: Macrocell with central macrocell BS and employed FAPs. Arrows indicate main radiation direction of the sector antennas, spaced out 120°.

B. Channel Model

- A power-law path loss model is used. Depending on the propagation environment, one of the following pathloss exponents is in force:
  - ◇ $\alpha = 4$ ... Outdoor environment
  - ◇ $\beta = 2$ ... Indoor area.
- The downlink signal experiences path loss and Rayleigh fading.
- Femtocells operate in Open Subscriber Group (OSG) mode. Users are assigned to a FAP or macrocell BS sector according to the highest average received power. Thus, the coverage area of a FAP can exceed the indoor area, as shown in Figure 1 (lower right FAP). On the other hand, indoor areas can partly be covered by nearby macrocell BSs (upper left FAP in Figure 1).
- Interference power typically dominates noise power in heterogeneous networks [4, 8]. Therefore, thermal noise is neglected in this work.

C. User Distribution (see Figure 2)

In order to generate hot-spot scenarios, users are distributed according to a Poisson cluster process [9], which is composed as follows:

1) A parent point process Φ uniformly spreads N_c circularly shaped areas of radius R_I over the coverage region of a macrocell sector.
2) A set of N_u users is distributed uniformly within each area.

The total amount of users in a macrocell sector is calculated as $N_c \cdot N_u$. By keeping this term constant, the parameters N_c and N_u adjust the *degree of clustering* (also referred to as extent of clustering, or level of inhomogeneity).

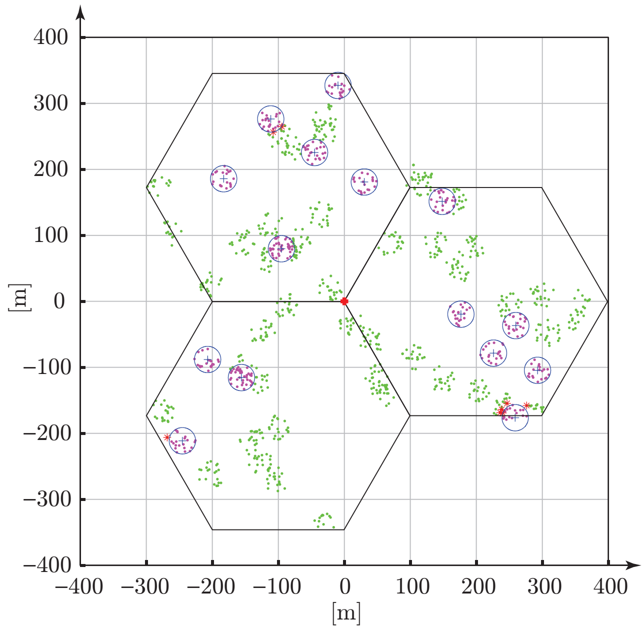

Fig. 2: Partial Femtocell Access Point deployment in clustered user scenario. The positions of users and FAPs are denoted by '·' and '+', respectively. Circles depict the indoor area of a femto-covered user-cluster; Outdoor users assigned to a FAP are marked by '∗'.

D. Notation and Conventions

- Macrocell BSs and FAPs are indexed by s and f, respectively. Index "0" labels the transmitter of the desired signal.
- The distance between user u and macrocell BS s (FAP f) is denoted by D_{us} (R_{uf}).
- The signal between user u and macrocell BS s experiences propagation loss:

$$\ell(D_{us}, \theta_{us}) = G_T(\theta_{us})\, D_{us}^{-\alpha},$$

  where $G_T(\cdot)$ denotes the angle-dependent radiation pattern of the employed sector antenna and θ_{us} is the angle between a user and the antenna's main radiation direction. The parameters D_{us} and α are the user-to-macrocell BS distance and the experienced path loss exponent, respectively.
- The Rayleigh fading coefficient is denoted as g_{us}, when related to macrocell BS sector s, and h_{uf}, when related to FAP f, respectively.

III. Signal-to-Interference Ratio Zones of the Partial Femtocell Deployment

In this section, we provide SIR expressions for a *partial* FAP deployment: A fraction of the user clusters is covered by FAPs, while the remaining part is under macrocell BS coverage, as depicted in Figure 2.

FAPs are placed at the center of randomly-chosen user clusters. We assume that wherever a FAP is operated, it is surrounded by an indoor area of size R_I and isolated from the outdoor environment by a wall with penetration loss L.

A user experiences one of the following interference situations:

1) It is located inside an indoor area and connected to the Femtocell Access Point. The SIR is obtained as:

$$\mathrm{SIR^i} = \frac{P_a R_{u0}^{-\beta} h_{u0}}{\sum\limits_{s\in\mathcal{S}} P_m \ell(D_{us},\theta_{us}) g_{us} L + \sum\limits_{f\in\mathcal{F}\setminus F_0} P_a R_{uf}^{-\alpha} h_{uf} L^2}, \tag{1}$$

where P_a and P_m denote the transmit power of a macrocell BS and a FAP, respectively. The term L is the wall loss, $\mathcal{S}$ denotes all transmitting sector antennas, $\mathcal{F}$ is the set of employed FAPs, and F_0 labels the transmitter of the desired signal. The signal from the interfering macrocell BSs experiences wall loss once (L), while the FAP interference experiences it twice (L^2).

2) Indoor users can also be assigned to a nearby macrocell BS, as indicated by the upper left FAP in Figure 1. The SIR then calculates as:

$$\mathrm{SIR^b} = \frac{P_m \ell(D_{u0},\theta_{u0}) g_{u0} L}{\sum\limits_{s\in\mathcal{S}\setminus S_0} P_m \ell(D_{us},\theta_{us}) g_{us} L + \sum\limits_{f\in\mathcal{F}} P_a R_{uf}^{-\alpha} h_{uf} L^2}, \tag{2}$$

with S_0 denoting the macrocell BS sector which provides the desired signal.

3) The remaining users are located outdoors. Depending on the strongest receive signal, they either communicate with the macrocell BS:

$$\mathrm{SIR^m} = \frac{P_m \ell(D_{u0},\theta_{u0}) g_{u0}}{\sum\limits_{s\in\mathcal{S}\setminus S_0} P_m \ell(D_{us},\theta_{us}) g_{us} + \sum\limits_{f\in\mathcal{F}} P_a R_{uf}^{-\alpha} h_{uf} L}, \tag{3}$$

or are handed off to a neighboring FAP:

$$\mathrm{SIR^o} = \frac{P_a R_{u0}^{-\alpha} h_{u0} L}{\sum\limits_{s\in\mathcal{S}} P_m \ell(D_{us},\theta_{us}) g_{us} + \sum\limits_{f\in\mathcal{F}\setminus F_0} P_a R_{uf}^{-\alpha} h_{uf} L}. \tag{4}$$

In the next section we evaluate the SIR expressions numerically.

IV. Numerical Results

A. Simulation Setup

In this setting, the cell cluster is composed of a center macrocell BS surrounded by six direct neighbors. The neighboring macrocell BSs are located on a hexagonal grid at a distance of 600 m. The antenna radiation pattern is referred from [10] and formulates as:

$$G_T(\theta) = -\min\left[12\left(\frac{\theta}{\theta_{3\mathrm{dB}}}\right)^2, A_m\right], \quad -180^\circ \le \theta \le 180^\circ, \tag{5}$$

with a 3 dB beamwidth of $\theta_{3\mathrm{dB}} = 65^\circ$ and maximum attenuation $A_m = 20$ dB.

A minimum coupling loss of 45 dB between FAP and user, and 70 dB between macrocell BS and user is taken into account [11]. The downlink signal experiences path loss and Rayleigh fading with unit average power. Further simulation parameters are listed in Table I.

Symbol	Description	Value
P_m	Macrocell BS transmit power	43 dBm[11]
P_a	FAP transmit power	13 dBm[11]
α	Outdoor path loss exponent	4
β	Indoor path loss exponent	2
L	Wall loss	20 dB
R_I	Indoor area radius	20 m
	Inter macrocell BS distance	600 m
	Tx × Rx antennas	1×1

TABLE I: Simulation Parameters

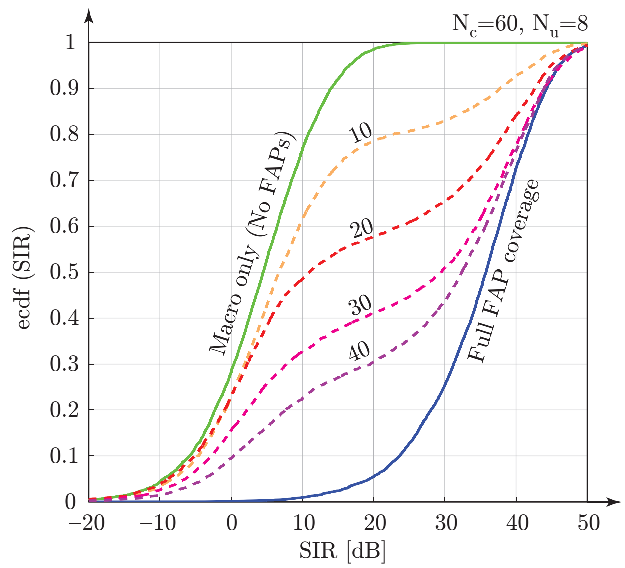

Fig. 3: SIR-ECDF curves for macrocell BS-only- (left solid line), fully FAP-covered- (right solid line) and partially FAP-covered scenario (dashed lines). Numbers denote the amount of employed FAPs.

Snapshots of a user hot-spot scenario are generated by first distributing N_c cluster centers uniformly over the coverage region of the macrocell BS. Then, N_u users are distributed uniformly around each cluster within a radius R_I. Simulation results are evaluated for users of the central macrocell (BS_0). The surrounding macrocells serve as interferers.

B. Signal-to-Interference Ratio Distribution

Figure 3 depicts the SIR distribution for various *partial* FAP deployments. The two extreme cases serve as a reference: (i) Leftmost solid line: No FAPs are employed. All users are assigned to the central macrocell BS and interference is caused only by the surrounding macrocell BSs. (ii) Rightmost solid line: All user-clusters are covered by FAPs. Interference is caused by the macrocell BSs (including the central one) as

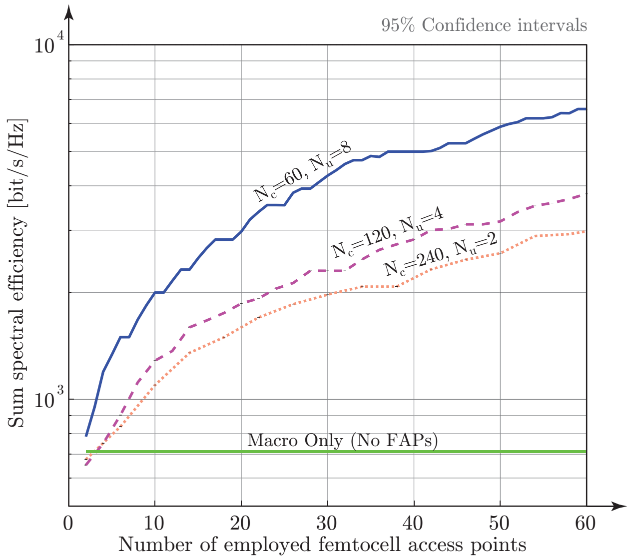

Fig. 4: Sum spectral efficiency of user scenarios from high (solid line) to low (dotted line) degree of clustering. N_c denotes the number of user clusters and N_u is the number of users per cluster.

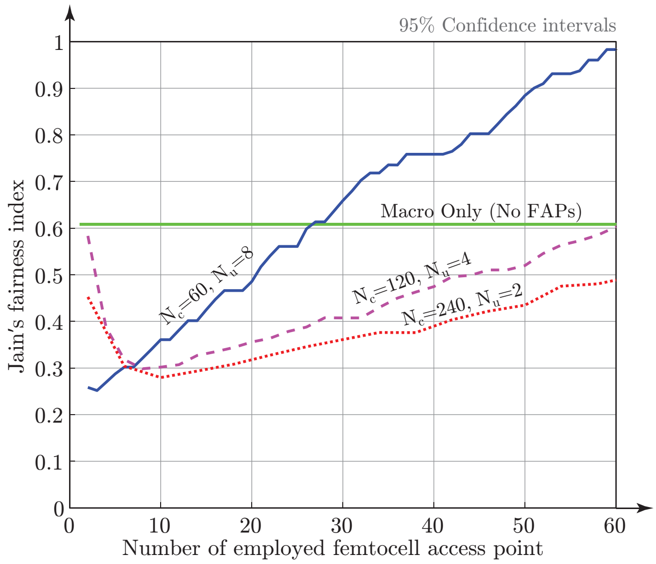

Fig. 5: Jain's fairness index: From high (solid line) to low (dotted line) degree of clustering. N_c denotes the number of user clusters and N_u is the number of users per cluster.

well as the other FAPs.

Dashed lines in Figure 3 correspond to the cases, when only a fraction of randomly-chosen user clusters is covered by FAPs (numbers denote the amount of employed FAPs). The step-like behavior of the curves indicate a large performance gap between macrocell- and femtocell users. By increasing the number of employed FAPs, the SIR curves of the partial FAP deployment tend towards the reference case of full FAP coverage. Thus, in terms of SIR it is beneficial to maximize the number of FAP-served user clusters. In the next subsection, we introduce sum spectral efficiency and fairness in order to quantify the efficiency of a femtocell-enhancement.

C. Sum Spectral Efficiency

Figure 4 depicts the sum spectral efficiency, calculated as

$$\sum_{\text{Users}} \log(1 + \text{SIR}_{\text{User}_i}), \tag{6}$$

versus the number of employed FAPs. Three scenarios are investigated, ranging from a high to a low degree of user clustering. Clustering is adjusted by varying the amount of clusters (N_c) and the number of users per cluster (N_u), while keeping the total amount of users $N_c \cdot N_u$ constant.

Sum spectral efficiency increases steepest in a user hot-spot scenario (solid line), and lowest in a close to uniform user distribution (dotted line), respectively. The results verify that the efficiency of femtocell operation is considerably dependent on the degree of clustering.

A second important effect is observed: When the number of employed FAPs is increased, the curves flatten due to the additional interference. This indicates a trade-off between femtocell deployment density and gain of sum spectral efficiency.

Sum spectral efficiency is suitable to measure the overall performance of a femto-enhanced network. However, it conceals the performance imbalance between macrocell- and femtocell users, as observed in Section IV-B (Figure 3). Therefore, we require measures which account for the distribution of spectral efficiency values among the users. We introduce a fairness index in the next subsection.

D. Fairness Index

In this paper, the widely used Jain's index serves to quantify the balance between macrocell- and femtocell user spectral efficiency. It is formulated as

$$f(\mathbf{t}) = \frac{\left(\sum_{i=1}^{N} t_i\right)^2}{N \sum_{i=1}^{N} t_i^2}, \tag{7}$$

where N is the total number of users in the network, and t_i denotes the spectral efficiency achieved by user i. Figure 5 depicts the fairness index plotted versus the number of FAPs employed in the macrocell.

In a sparse femtocell deployment (i.e., low number of FAPs), only few users achieve high spectral efficiency values due to their vicinity to the FAP. The remaining users are attached to the macrocell BS and experience additional interference from the femtocells. Therefore, low fairness is achieved. The fairness index increases with the number of employed FAPs and takes on its maximum at full femtocell coverage, i.e. all user clusters are covered by a FAP. In this case, the spectral efficiency values of the users are most balanced. The results show that efficient balancing of user spectral efficiency is only possible in scenarios with a high degree of clustering. In close to uniform distributions, the achieved fairness of a femto-enhancement does not exceed the reference case without FAPs.

V. Summary and Outlook

In this paper, the efficiency of Femtocell Access Point (FAP) deployments in a macrocellular network was investigated. We focused on the influence of the user distribution, in particular the degree of user-clustering. A sectorized cell layout was used to carry out numerical evaluations.

Results verify that FAPs operates most efficiently in a user hot-spot scenario with high degree of user-clustering. Compared to a scenario without femtocells, a femto-enhancement always improves sum spectral efficiency. However, our findings emphasized that this metric conceals the distribution of individual user performance. Therefore, we introduced Jain's fairness index. We showed that fairness improvement with regard to the non-femtocell enhanced reference network requires a minimum degree of user-clustering.

Our method can be applied to assess the efficiency of femtocell-enhancements in real world scenarios. The required knowledge about the degree of user-clustering is obtained from metrics as the ones defined in [12, 13].

Acknowledgments

The authors would like to thank the LTE research group for continuous support and lively discussions. This work has been funded by KATHREIN-Werke KG and A1 Telekom Austria AG.

References

[1] F. Baccelli and B. Błaszczyszyn, *Stochastic Geometry and Wireless Networks, Volume I and II*, ser. Foundations and Trends in Networking. NoW Publishers, 2009.

[2] H. S. Dhillon, R. K. Ganti, F. Baccelli, and J. G. Andrews, "Modeling and Analysis of K-Tier Downlink Heterogeneous Cellular Networks," *CoRR*, vol. abs/1103.2177, 2011.

[3] M. Haenggi and R. K. Ganti, *Interference in Large Wireless Networks*, ser. Foundations and Trends in Networking. NoW Publishers, Feb. 2009, vol. 3.

[4] H.-S. Jo, Y. J. Sang, P. Xia, and J. G. Andrews, "Heterogeneous Cellular Networks with Flexible Cell Association: A Comprehensive Downlink SINR Analysis," *CoRR*, vol. abs/1107.3602, 2011.

[5] J. Andrews, F. Baccelli, and R. Ganti, "A Tractable Approach to Coverage and Rate in Cellular Networks," *Communications, IEEE Transactions on*, vol. 59, no. 11, pp. 3122 –3134, Nov. 2011.

[6] V. Chandrasekhar, J. Andrews, and A. Gatherer, "Femtocell Networks: A Survey," *Communications Magazine, IEEE*, vol. 46, no. 9, pp. 59 –67, Sept. 2008.

[7] H.-S. Jo, P. Xia, and J. G. Andrews, "Open, Closed, and Shared Access Femtocells in the Downlink," *CoRR*, vol. abs/1009.3522, 2010.

[8] N. Jindal, J. G. Andrews, and S. Weber, "Energy-Limited vs. Interference-Limited Ad Hoc Network Capacity," in *Proceedings of the 41st Annual Asilomar Conference on Signals, Systems, and Computers*, Nov 2007.

[9] D. Stoyan, W. Kendall, and J. Mecke, *Stochastic Geometry and its Applications*. Wiley Series in Probability and Statistics, 1995.

[10] 3GPP, "Evolved Universal Terrestrial Radio Access (E-UTRA); Radio Frequency (RF) System Scenarios," 3rd Generation Partnership Project (3GPP), TS 36.942, Dec. 2010.

[11] ——, "Base Station (BS) Radio Transmission and Reception (FDD)," 3rd Generation Partnership Project (3GPP), TS 25.104, Dec. 2011.

[12] U. Schilcher, M. Gyarmati, C. Bettstetter, Y. W. Chung, and Y. H. Kim, "Measuring Inhomogeneity in Spatial Distributions," in *Vehicular Technology Conference (VTC) Spring 2008*, May 2008, pp. 2690 –2694.

[13] P. M. Dixon, "Ripley's K Function," in *Encyclopedia of Environmetrics*. John Wiley & Sons, Ltd, 2001. [Online]. Available: http://dx.doi.org/10.1002/9780470057339.var046